Microsc. Microanal. 10, 1–16, 2004
DOI: 10.1017/S1431927604040942

Microscopy AND Microanalysis

New Approaches to the Microscopic Imaging of *Trypanosoma brucei*

Mark C. Field,[1,*] Clare L. Allen,[1] Vivek Dhir,[1] David Goulding,[1] Belinda S. Hall,[1] Gareth W. Morgan,[1] Paul Veazey,[1] and Markus Engstler[2]

[1]*Wellcome Trust Laboratories for Molecular Parasitology, Department of Biological Sciences, Imperial College, Exhibition Road, London SW7 2AY, UK*
[2]*Ludwig-Maximilians-Universitaet, Department Biologie I, Genetik, Maria-Ward-Str. 1a, 80638 Muenchen, Germany*

Abstract: Protozoan parasites are fearsome pathogens responsible for a substantial proportion of human mortality, morbidity, and economic hardship. The principal disease agents are members of the orders Apicomplexa (Plasmodium, Toxoplasma, Eimeria) and Kinetoplastida (Trypanosomes, Leishmania). The majority of humans are at risk from infection from one or more of these organisms, with profound effects on the economy, social structure and quality of life in endemic areas; Plasmodium itself accounts for over one million deaths per annum, and an estimated 4×10^7 disability-adjusted life years (DALYs), whereas the Kinetoplastida are responsible for over 100,000 deaths per annum and 4×10^6 DALYs. Current control strategies are failing due to drug resistance and inadequate implementation of existing public health strategies. *Trypanosoma brucei*, the African Trypanosome, has emerged as a favored model system for the study of basic cell biology in Kinetoplastida, because of several recent technical advances (transfection, inducible expression systems, and RNA interference), and these advantages, together with genome sequencing efforts are widely anticipated to provide new strategies of therapeutic intervention. Here we describe a suite of methods that have been developed for the microscopic analysis of *T. brucei* at the light and ultrastructural levels, an essential component of analysis of gene function and hence identification of therapeutic targets.

Key words: *Trypanosoma*, protein transport, vesicle trafficking, endocytosis, fluorescence microscopy, ultrastructure

Introduction

Trypanosoma brucei, a digenetic unicellular hemoflagellate of the order Kinetoplastida, is the causal agent of human sleeping sickness in sub-Saharan Africa. In endemic areas tens to hundreds of thousands of individuals are infected each year and trypanosomiasis is probably responsible for more deaths than HIV infection in such locales. Overall the parasite kills 100,000 individuals per annum and is responsible for morbidity of 4×10^6 disability-adjusted life years (DALYs) (Remme et al., 2002; http://www.who.int/tdr/). Most critically, health agencies have essentially lost control of the disease in the last half century due to social and geopolitical problems; resultant poor public health implementation has resulted in widespread emergence of drug resistance (Legros et al., 2002). In addition to human disease, infection of domestic cattle by *T. brucei* has an enormous, but poorly quantified, negative impact on human welfare as it is difficult to rear cattle in endemic areas, where use of bovines as draught animals is frequently the only agricultural strategy available.

In addition to being the cause of disease and economic burden, *T. brucei* represents a very important model system for molecular cell biology, genetics, and biochemistry (Beverley, 2003). Indeed, as a highly divergent eukaryote, it provides a unique perspective on the biology of the eukaryotic lineage, and has now matured into an excellent model system (Gull, 1999). Study of *T. brucei* at the molecular level has led to numerous discoveries about basic processes in cells, including the first molecular descriptions of immune evasion via antigenic variation (Cross, 1996), *trans*-splicing and polycistronic transcription in an eukaryote (Agabian, 1990), RNA editing (Kable et al., 1997), compartmentalization of glycolytic enzymes (Opperdoes & Michels, 1993), and GPI anchors on cell surface proteins (Ferguson, 1999). Hence, study of *T. brucei* accesses unique aspects of biology, such as immunological evasion mechanisms, metabolic control, gene expression systems, intracellular transport, and flagellar motility, several of which cannot readily be explored in other experimental models.

Despite the unavailability of a number of stages *in vitro*, two of the major proliferative stages are routinely

Received January 20, 2003; accepted April 7, 2003.
*Corresponding author. E-mail: mfield@ic.ac.uk

grown in the laboratory in semidefined media. These are the insect gut stage, known as the procyclic form (PCF) and the bloodstream long slender stage (BSF). These two forms are quite distinct; for example, the PCF has an active mitochondrion, whereas the BSF has residual mitochondrial function, and the PCF surface coat consists of acidic repeat proteins (procyclins) whereas the BSF is covered by globular neutral proteins, variant surface glycoproteins (VSG) (McConville & Ferguson, 1993; Ferguson, 1999). Substantial alterations in phospholipid composition have also been reported (Patnaik et al., 1993), and together these substantive developmental alterations have a significant impact on the methodology that must be employed when studying these cells. In addition, the terminally differentiated insect-infective stumpy form can also be generated *in vitro*. However, over the last decade considerable progress has been made in morphological study of *T. brucei*, including the use of live cell imaging and the description of an increasing number of proteins providing intracellular markers. Here we detail methods for the localization of antigens by immunochemical methods and marking of intracellular compartments with live cell fluorescence reagents and lectins, as well as discussing technical pitfalls that may arise.

Morphology and the Location of Compartments in *T. brucei*

The African trypanosome is a highly polarized spindle-shaped cell, approximately 18–20 μm long and 3 μm thick (Fig. 1). By phase-contrast microscopy, the cells are highly motile in culture, varying between a C and S shape, with a clearly visible flagellum running the length of the cell body; the flagellum emerges from the cell body close to the cell posterior. Rapid sinusoidal undulations of the flagellum serve to propel the cell through the medium. The most prominent intracellular organelle visible by phase is the nucleus, which is typically positioned at the midpoint of the cell; additional smaller phase dark and light structures may be visible in the cytoplasm, which likely correspond to organelles of the endomembrane system and acidocalcisomes.

A description of the trypanosome cell form is in Hoare (1972), which provides an excellent introduction to this topic. The first well-documented morphological descriptions of African trypanosomes were by Minchin (1909) and Bruce (1911). Bruce, in particular, was highly aware of the importance of morphology, and his series of Croonian Lecture's published in the Lancet pay particular attention to this aspect of trypanosome biology (Bruce, 1915). The cytology of these organisms was highly controversial in the earlier literature, with the function and composition of the organelles visible at that time being strongly contested. Morphological variation is a common feature, even under controlled axenic culture conditions (e.g., Tyler et al., 2001), which may well have contributed to this debate. A widely known major error in the classification of trypanosome subcellular structures was the kinetoplast, the defining feature of the entire order. As its name implies, this organelle was originally considered as part of the locomotory apparatus, because of its association with the base of the flagellum; however, it is now known to be the mitochondrial DNA, and probably associated with the basal body to ensure correct segregation at mitosis (Lukes et al., 2002; Wang et al., 2002). The first detailed studies at the ultrastructural level were by Vickerman (1969*a*, 1969*b*, 1970). Significantly, the first reports that trypanosomes possessed a pinocytotic system date from about this time (Armstrong et al., 1964), a concept suggesting that the organism may have a specialized feeding system. Previously, trypanosomes were considered to be saprozoic (Hoare, 1972).

Simple fixation and staining for DNA (most usually using DAPI) reveals additional polarity in the cell; the nucleus occupies the central region, its center usually roughly 50% of the distance from the posterior to the anterior end. Fortuitously, the cell is somewhat flattened following fixation and the trypanosome comes to lie on one side, such that the flagellum is positioned along one edge of the cell, with the internal structure unobscured (Hoare, 1972). The nucleus is approximately 1.5 μm in diameter, and is a clear oval in the procyclic form, but rather more flattened in the BSF (Rout & Field, 2001). The second prominent structure that is visualized by DAPI stain is the kinetoplast. The relative position of the kinetoplast and nucleus alter, depending on the developmental stage; in the procyclic the kinetoplast is closer to the posterior end of the cell than the nucleus, but in the BSF the opposite is true (Hoare, 1972). The kinetoplast provides a particularly useful cell marker, as it is easy to fix and stain, is located close to the flagellum basal body and the flagellar pocket, and replicates in a coordinate fashion with the nucleus, as first described in detail by Gull and coworkers (Robinson et al., 1995; Gull, 1999). Specifically, when *T. brucei* enters mitosis, the kinetoplast initiates replication early ($K_1N_1 \rightarrow K_2N_1$),[1] followed by replication of nuclear DNA (K_2N_2). The kinetoplasts divide first and migrate at this stage so that the order of organelles is KNKN (posterior to anterior). This process is then followed by cytokinesis, with growth of the cleavage furrow between the central N and K, to regenerate the interphase state (Robinson et al., 1995). Additional organelles, most prominently the Golgi complex, replicate in a coordinate manner with the kinetoplast (Field et al., 2000), making *T. brucei* an attractive system for the study of cell cycle and organelle inheritance.

Further information, provided by a combination of ultrastructure and immunofluorescence, has demonstrated that the majority of the endomembrane system is localized between the nucleus and kinetoplast, presumably reflecting

[1]In this instance, K = kinetoplast and N = nucleus. The subscripts denote the number of organelles, and not the ploidy of the genome.

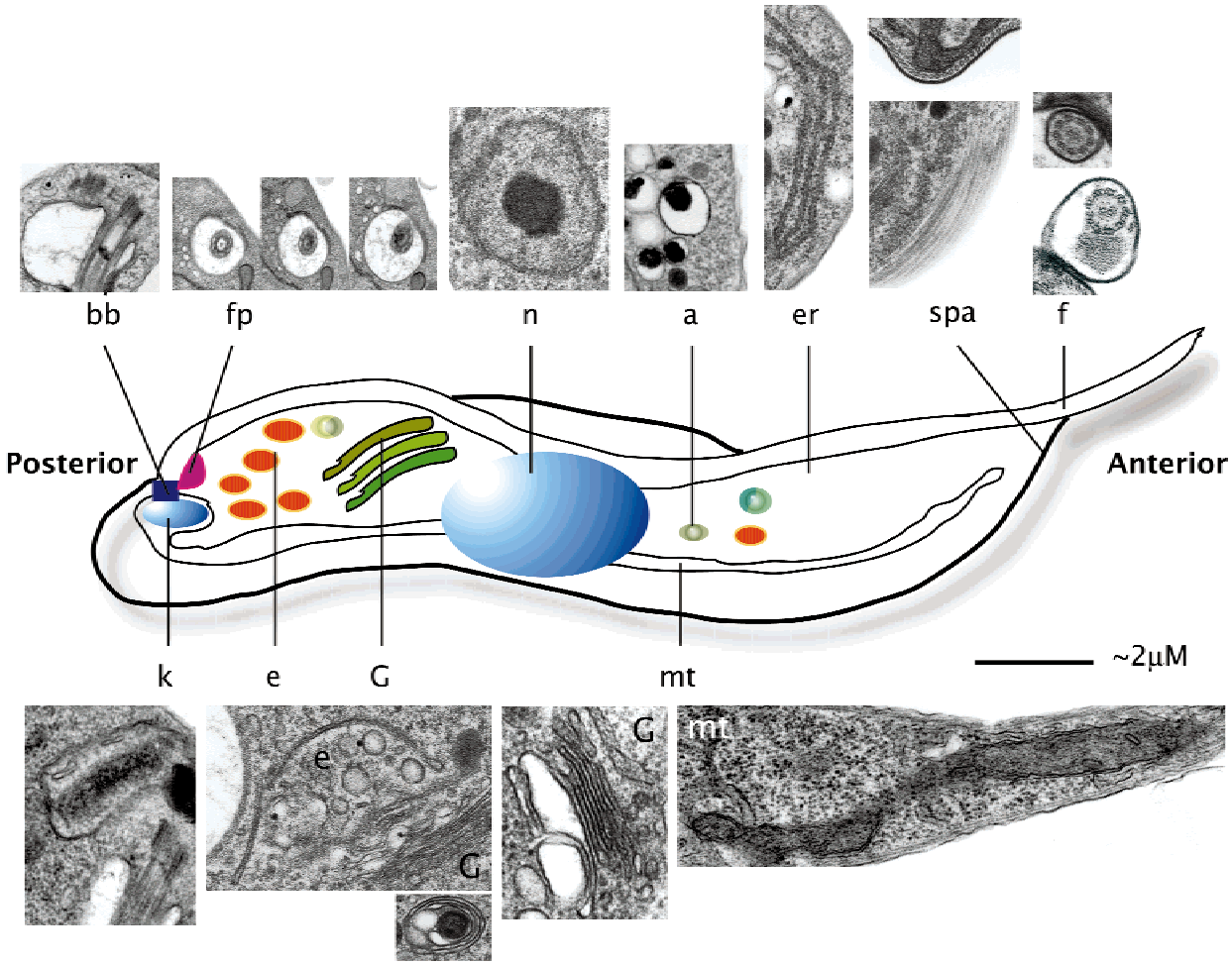

Figure 1. Schematic of the trypanosome cell. The central image is a cartoon showing the locations of the major organelles and structures. The endoplasmic reticulum (er) has been omitted for clarity as this structure extends throughout the cell and also forms the nuclear envelope. Structures shown are: a: acidocalcisome; fp: flagellar pocket; bb: basal body; n: nucleus; spa: subpellicular microtubule array; f: flagellum; k: kinetoplast (mtDNA); e: endosomes; G: Golgi complex; mt: mitochondrion; and er: endoplasmic reticulum. The insets show examples of these structures as seen by thin-section transmission electron microscopy. For the basal body, note the presence of the structure as it passes through the flagellar pocket membrane. Three serial section images of the fp are shown; at this level the flagellum lacks the paraflagellar rod, which normally supports the axoneme. The image of the nucleus (n) illustrates the double membrane surrounding the organelle, together with the single prominent electron-dense nucleolus. Acidocalcisomes are observed as electron dense structures within the cytoplasm, but in thin-section mounts the luminal contents are often partially or fully lost, resulting in apparently empty structures. Three closely apposed rough ER membranes are shown. The subpellicular microtubule array (spa) is shown in both transverse (top) and glancing (bottom) section; note the highly ordered periodicity of this cytoskeletal component that is responsible for maintaining the overall shape of the organism. Two transverse sections though the flagellum are shown, one at the level of the flagellar pocket (top) and lacking a paraflagellar rod, and a second higher up, where the flagellum contains the axoneme and paraflagellar rod. Note the presence of the electron dense membrane associated with the flagellum-contact zone on the flagellar pocket. The kinetoplast (k) is observed as a thick electron-dense disc of material (in this example in transverse section). The kinetoplast is enclosed in the mitochondrial membrane and is in close association with the base of the flagellum. The endocytic and secretory apparatus of the Golgi complex (G) and endosomes (e) are also closely associated; endosomes close to the flagellar pocket are indicated, as is a Golgi stack (G). A second prominent Golgi complex is also shown. At the bottom a multivesicular endosome is shown. Finally, a section through a portion of the single mitochondrion (mt) in the anterior portion of a procyclic cell is shown. The posterior and anterior ends of the cell are also indicated.

the important role of the flagellar pocket in both secretion and endocytosis as well as the polarity of the cytoskeleton (reviewed in Morgan et al., 2002*a*, 2002*b*). Thus, the Golgi complex (which is more extensive in the bloodstream stage compared to the procyclic form; Field et al., 2000), the single lysosome (Bangs, 1998) and the endosomes (reviewed in Morgan et al., 2002*b*; Overath & Engstler, 2004) are all located in this posterior region of the cell. By contrast, the endoplasmic reticulum (ER), the mitochondria, and the glycosomes are all dispersed throughout the cell volume (Bangs et al., 1996; Vassella et al., 1997; Lorenz et al., 1998; Ali et al., 1999). Both the ER and the mitochondria form contiguous but distinct networks, so that no part of the cytoplasm is far form these organelles. Acidocalcisomes are distributed throughout the cytoplasm, with no apparent polarity (Docampo & Moreno, 1999). Although there is no contractile vacuole, and *T. brucei* appears unable to osmoregulate, recent evidence points to an evolutionary relationship between the contractile vacuole and acidocalcisomes (Marchesini et al., 2002).

Instrumentation Considerations

For a cell that is less than 20 μm $\times$ 5 μm, the primary consideration must be resolution. The two major forms of fluorescence microscope are confocal or wide field. The choice depends on the sample, and for *T. brucei*, this decision appears simple. The major advantage of confocal is relatively deep optical penetration, that is, the possibility to work with specimens that are up to hundreds of micrometers thick. *T. brucei*, however, is translucent and anything but thick, and the confocal microscope is disadvantageous. Wide-field microscopes also have an up to 1000-fold better signal-to-noise ratio and do not rely on a few laser lines for fluorescence excitation. Especially for imaging of live trypanosomes, it is desirable to adjust the light energy for maximum fluorescence intensity and minimum photo damage of the cells, a difficult task for a confocal setup but easily achieved with wide field. The speed of image acquisition of wide-field systems is only limited by the performance of the charge coupled device (CCD) camera. High-end cameras allow much faster image acquisition than any serial or line scanner of a confocal microscope. Thus, for live cell analysis, or for low abundance antigens, a wide-field microscope, equipped with a very fast, high-resolution, cooled CCD camera, and robust, real three-dimensional deconvolution software produces superior results.

A standard-build high-quality epifluorescence microscope, from Nikon, Zeiss, or Olympus is a good choice for the optical stage. In the past few years, excellent high-magnification objectives have been produced by all of these companies (e.g., both Nikon and Zeiss supply a 100$\times$ objective), which has had a very positive impact on imaging of trypanosomes. An image doubler and DIC are important add-ons after a standard set of fluorescence filter blocks. It is important to ensure that all filter blocks are optically matched for dual channel analysis. The most critical aspect of a system, however, resides in the camera system. There are many excellent CCD cameras available, and different workers will express preferences for one vendor over another. We have found that cooled CCDs from Photometrics LLC provide excellent sensitivity (low dark current is essential for detection of weak signals) and resolution. Ongoing advances with CCD technology mean that any detailed discussion of this topic is bound to be out of date rapidly. Such a system is financially within the reach of most laboratories. The DeltaVision system (www.api.com/products/bio/deltavision.html), which incorporates both high build quality and a number of innovations including highly uniform sample illumination, does provide an appreciable increase in data quality over conventional wide-field fluorescence, but this is a somewhat more expensive system.

Finally, there are numerous choices for software controllers for fluorescence systems, including IPLab (www.scanalytics.com), Lucia (www.lim.cz), Metamorph (www.image1.com), and Image Pro Plus (www.mediacy.com) as well as numerous free solutions. The choice is mainly dependent on the preferred operating system, the complexity of the studies to be undertaken, and compatibility with the chosen camera. For example, Metamorph (for Windows PC [www.microsoft.com]) or IPLab (for Macintosh [www.apple.com]) are very powerful suites of programs, with a modular architecture that allows scripting (IPLab) and new functionality to be added as required. All of these software solutions are in continual development, and again selection is quite personal as all will cover the basic tasks of camera control and image acquisition adequately. Subsequent image manipulation capabilities vary between these systems, and in addition all will provide data that can be migrated into standard image assembly packages such as Adobe Photoshop (www.adobe.com) or the free NIH Image (rsb.info.nih.gov/nih-image/). The latter is particularly good for quantitation, but for high-end use much analysis may be automated by Metamorph or IPLab and would therefore be recommended. Professional volume, surface rendering, and measurement tools include the Imaris Surpass+modules (www.bitplane.ch).

Deconvolution: Any image is nonequivalent to the real object, and in biological microscopy this basic aspect of physics can be a major difficulty. In particular the optics of the microscope alter the appearance of the imaged specimen. Thus, the real object is folded, or more formally "convolved," resulting in a blurred image. All factors that contribute to the convolution (mathematical sign: $\otimes$) of a microscopic system are summarized by the point spread function (PSF). If the PSF is known it is possible to reverse the convolution, that is, deconvolution ($\otimes^{-1}$) and unfold the imaged object by mathematical algorithms that utilize a calculated or measured PSF. Ideally, the result is a deblurred image with a true increase in axial and lateral resolution. For small objects, such as trypanosomatids, the resolution

issue is particularly critical, and hence any method that can improve image quality is a major advantage.

Three major classes of deconvolution algorithms are available. Nearest neighbor algorithms are very fast, but should be considered as "unsharp masking" or three-dimensional (3D) sharpening filters, rather than as true 3D deconvolution algorithms. Inverse convolution algorithms are fast and based on true 3D methods. However, these do not lead to a true increase in image resolution. The best choice is a group of high-end algorithms that guarantee reliable results and a significant increase in 3D image resolution. Among these "Constrained, Iterative Deconvolution Algorithms," van Cittert, Maximum Entropy, Iterative Constrained Tikhonow–Miller, and Maximum Likelihood Estimation are most widely used. These algorithms, however, require patience from the researcher and a lot of memory and fast CPUs from the computer hardware. Professional deconvolution systems (e.g., the Huygens System; www.svi.nl) are capable of handling multiple, four-dimensional multichannel images of arbitrary size at the same time. The PSF can either be calculated using electromagnetic diffraction-based PSF generators or it is experimentally derived from finite sized microsphere images.

In addition, it is most important to account for non-static variables, such as lamp jittering or fluorescence fading. Although modern deconvolution software will recognize and correct even those parameters, an oversampling two-fold smaller than the lateral and axial resolution of the microscopic system is required. When digital deconvolution is done in an expert way, the results can provide new insights into the subcellular architecture and, more importantly, will yield data that reliably can be used for quantitative and qualitative description of the sample.

Marker Proteins and Reagents for *T. brucei* Organelles

The availability of well-defined markers for subcellular compartments for trypanosomes has been much improved over the last few years, due in part to genome sequencing, but probably more importantly from maturation of the field, and the emergence of a true trypanosomatid molecular cell biology. This has served to refine and, in some instances redefine, compartments that were originally described based on a behavioral property, but can now be characterized by the presence of a molecular marker (e.g., the collecting tubules have now been equated to the early/recycling endosomes, in homology with other eukaryotic systems; Jeffries et al., 2001). In addition, several commercial stains have been successfully exploited in the trypanosome system, for example, MitoTracker and Bodipy-Ceramide (Vassella et al., 1997; Denny et al., 2000), where they behave in a manner essentially indistinguishable from higher eukaryotes. A list of recommended antibodies and stains is provided in Table 1. The majority of these are discussed in more detail in the following sections. Some are illustrated in Figures 2–5.

Methodology

Described in the following sections is a selection of methods for the analysis of *T. brucei* by microscopy. The main focus here is on methodology that is likely to be generally applicable, and of utility, to a wide audience. Hence, highly specialized procedures, which require either extensive training or specialized (and expensive) infrastructure, have not been included.

Fixation and Preparation of Trypanosomes for Immunofluorescence Analysis (IFA)

Procyclic (PCF) or bloodstream (BSF) parasites in exponential growth (1×10^7 cells/ml for PCFs and 1×10^6 cells/ml for BSFs) are harvested by centrifugation for 10 min at $800 \times g$. Pelleted parasites are resuspended in ice cold Voorheis's modified PBS (vPBS; 137 mM NaCl, 3 mM KCl, 16 mM Na_2HPO_4, 3 mM KH_2PO_4, 46 mM sucrose, 10 mM glucose, pH 7.6; Nolan et al., 2000) and centrifuged again at $800 \times g$ for 10 min. The cell pellet is then gently resuspended in vPBS at 2×10^7 cells/ml. An equal volume of 6% paraformaldehyde (w/v) prepared in vPBS is then added and the cells fixed for either 1 h (PCFs) or 10 min (BSFs) on ice. Following fixation, the fix solution is diluted by adding fivefold excess vPBS and the paraformaldehyde removed by first pelleting the cells ($800 \times g$ for 5 min) and then washing once with vPBS. The final pellet is resuspended at 2×10^7 cells/ml in vPBS and applied to a 0.2×0.2 cm area, drawn using a PAP pen (Sigma), to poly-lysine slides (Sigma) in 150-μl aliquots and allowed to settle for 20 min.

To stain internal structures the parasites are permeabilized in PBS (137 mM NaCl, 3 mM KCl, 16 mM Na_2HPO_4, 3 mM KH_2PO_4), 0.1% Triton X-100 for 10 min, before the slides are washed three times with excess PBS. After this wash, 250 μl of block solution (20% FCS) is applied to the cells for an hour at room temperature. Subsequent to blocking, 200 μl of primary antibodies are added at their correct working dilutions (diluted in 20% FCS in PBS) and slides incubated for 1 h at room temperature. The slides are then washed three times in PBS each for 5 min at room temperature, following which 250 μl of fluorophore (Texas Red, FITC, Alexa) conjugated secondary antibodies (Molecular Probes), specific to the species in which the primary antibody is raised, are added at the relevant dilution (in 20% FCS) and slides incubated for 1 h. Subsequently, slides are washed three times in PBS for 5 min. Excess PBS is carefully removed and 2 μl of mount (1 mg/ml 4′,6′-diamidino-2-phenylindole in Mowiol; Calbiochem) is applied to the cells to visualize DNA and preserve fluorophore activity. A coverslip is then immediately applied and sealed in place using

Table 1. Molecular Markers for Subcellular Compartments and Structures of Interest in *T. brucei*[a]

Compartment	Reagent	Target[b]	Reference
ER	Anti-TbBiP[c]	BiP	Bangs et al., 1996
Golgi	Bodipy-Ceramide	Lipid domains	Field et al., 2000
	Anti-TbRAB18[d]	Rab18	Jeffries et al., 2002
	Anti-TbRAB31	Rab31	Field et al., 2000
Endosomes	Anti-ISG_{100}[d]	ISG_{100}	Nolan et al., 1999
	Anti-TbRAB5A	Rab5A	Field et al., 1998
	Anti-TbRAB11	Rab11	Jeffries et al., 2001
	FM 4-64[e]	Lipid membranes	B.S. Hall, A. Acosta-Serrano, & M.C. Field, submitted
	Transferrin[f]	Transferrin receptor	
Late endosomes	Anti-TbRAB7	Rab7	Engstler et al., 2004
Lysosome	CB-1/Anti-p67	p67	Kelley et al., 1999
	LysoTracker	pH	P. Veazey & M.C. Field, unpubl.
Flagellar pocket	Concanavalin A[g]	Glycoproteins	Balber & Frommel, 1988
Mitochondria	Mitotracker	ΔpH gradient	Ali et al., 1999
Glycosome	Anti-TbPEX11	TbPEX11	Lorenz et al., 1998
Nuclear envelope	Anti-NUP-1	NUP-1	Ogbadoyi et al., 2000; Rout & Field, 2001
Nucleus and kinetoplast	DAPI	DNA	
Nucleolus	Anti-NUMAG	NUMAG	Ogbadoyi et al., 2000
Basal body	BBA4 Mab	Not known	Woodward et al., 1995
Plasma membrane	Anti-VSG[d]	VSG	Various
	Anti-Procyclin	Procyclin	

[a]This list is not exhaustive, and as new markers and factors are identified, the reagent of choice is likely to alter. However, at the time of writing, the stains and markers suggested are the most reliable available. The list also includes common commercially available stains for trypanosome subcellular compartments. Numerous fluorophores are available for the specific staining of subcellular compartments of eukaryotic cells. Only a subset of these have been successfully utilized and reported in the literature for trypanosomes. All of the listed reagents have been verified by ultrastructure, colocalization with an authenticated marker, or other robust means. Protocols for the use of these compounds are described in the text.

[b]Molecular target (protein) or process that is used to stain the organelle/compartment under consideration.

[c]BiP is a high-abundance chaperone molecule of the ER.

[d]Only suitable for use in the bloodstream-form stage.

[e]This reagent is most useful as a measure of membrane internalization.

[f]Transferrin binds to *T. brucei* via the ESAG6/7 GPI-anchored heterodimeric transferrin receptor. Recent work has demonstrated a recycling pathway for the ligand, which also involves extensive degradation, and only a portion of the pathway is visualized in fixed cells.

[g]Depending on the conditions employed, Concanavalin A may be used to mark the flagellar pocket, the early endocytic system, and the late endocytic system/lysosome. Similarly, Bodipy Ceramide stains both the Golgi complex and the ER; differential staining can be easily achieved. See text for details.

nail varnish, before visualization. For a simple mount where only the location of the nucleus and kinetoplast is required, the cells are permeabilized, washed, and then mounted immediately, omitting the intermediate steps for antibody staining. An example is shown in Figure 5; note that here, the cells are expressing a protein ectopically (TbRAB2); despite these cells being derived from a clone, the staining intensity is nonuniform, in marked contrast to the endogenous tubulin stain (Field et al., 1999). The basis for this phenomenon has not been explained, but does add an additional level of complexity to the analysis of transgenic trypanosomes.

Costaining with Primary Antibodies of the Same Species

A common problem when attempting to colocalize two antigens is the situation where both primary antibodies are derived from immunization of the same species, that is, two polyclonal sera from rabbits or two mouse monoclonals. Several methods have been devised for this, including the removal of any excess secondary antibody with excess nonimmune serum from the primary animal species, and although this methodology can work well (Field et al., 1998), it is not completely reliable in all workers' hands.

An excellent alternative is the Zenon™ technology recently developed by Molecular Probes. This kit efficiently labels each rabbit antibody with the desired fluorophore; thus there is no requirement for a labeled species-specific secondary antibody. In addition there is no requirement for covalent attachment of a fluorophore, which is technically demanding with the small quantities of material frequently available. The protocol is as described above for standard labeling to the point at which blocking solution is applied. During the blocking reaction, each rabbit antibody (1 μg)

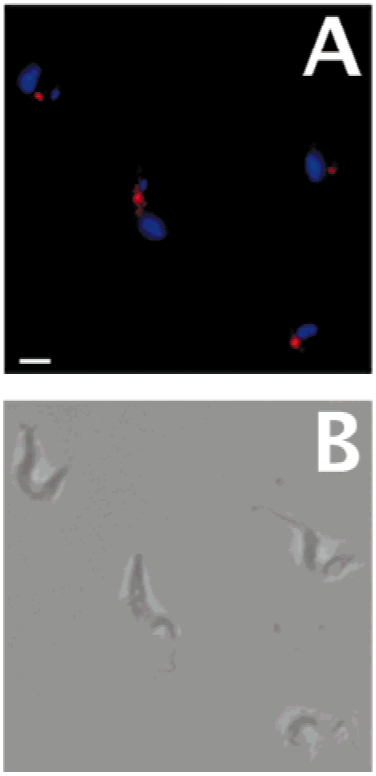

Figure 2. *See caption on facing page.*

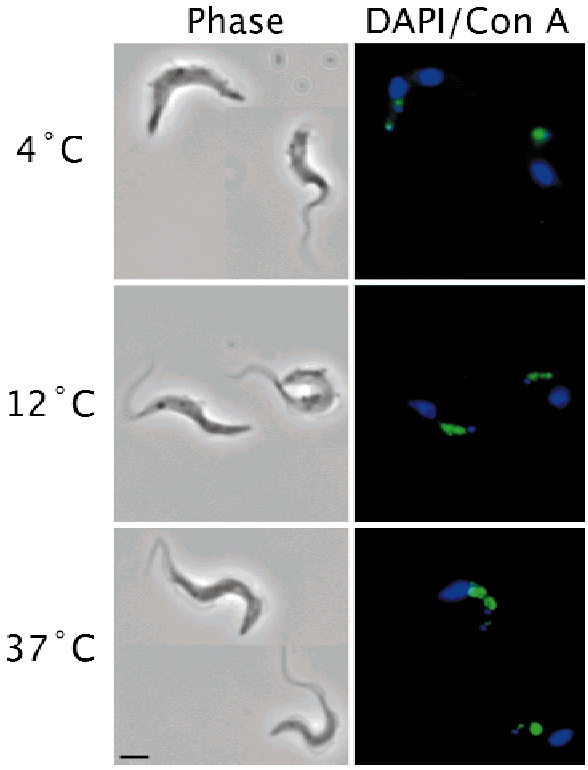

Figure 4. *See caption on facing page.*

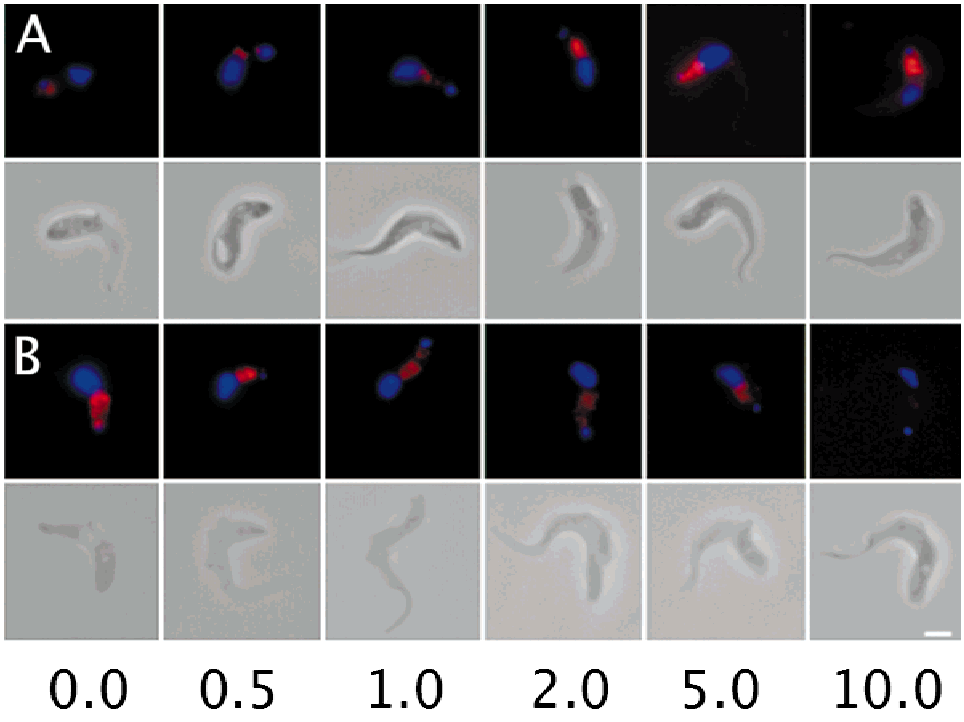

Figure 3. *See caption on facing page.*

to be labeled is incubated with 5 μl of the desired fluorophore (blue, green, or red as supplied with the kit) for 10 min in the dark at room temperature. Following this incubation, 5 μl of Zenon block (supplied with the kit) is added and the reaction stored at room temperature for 5 min to clean the reaction of any excess label. This is then immediately applied (250 μl of each antibody) at a dilution (in 20% FCS) fivefold higher than it is used under standard labeling conditions to the slides (from which the block has been removed). The slides are incubated for an hour before they are washed three times, each wash lasting 5 min, in excess vPBS. To the slides, 250 μl of ice cold 3% paraformaldehyde is applied for 1 min and rapidly washed off in excess PBS three times. The slides are then mounted as described above and visualized immediately for the best results.

Special Considerations for Working with Delicate Cells

A number of knock-out and RNA interference strains exhibit phenotypes in which, for one reason or another, the structural integrity of the cell has been compromised to some extent, with the result that morphology is poorly preserved following processing. The major consideration when working with such delicate cells is to keep the number of manipulations to an absolute minimum. Although this may increase background staining, when offset against extreme losses and damage of cells in the sample, this is frequently an acceptable compromise. In particular, multiple wash steps can result in damage or loss of fragile cells due to centrifugation (Allen et al., 2003). However, if centrifugation steps cannot be avoided, cell damage can also be reduced in several ways. First, centrifugation should be performed at the slowest speed possible in the worker's centrifuge to enable the cells to pellet and without using the brake. The use of Voorheis's modified PBS instead of PBS as a wash buffer also helps to reduce damage to the cells as the high sucrose content in this buffer provides an osmotic cushioning effect, as well as additional nutrients in the case of bloodstream form cells. To prevent further mechanical damage the cell pellet should not be resuspended by pipetting during the wash steps, but rather by very gentle agitation. Finally $\sim 3\times$ the number of fragile cells should be used for any assay involving several centrifugation steps to allow for loss of cells. For IFA, the cells can be fixed directly in culture prior to any centrifugation steps by adding 37% formaldehyde at a 1:10 dilution. Once the cells have fixed they should be more stable for centrifugation; however, the use of formaldehyde rather than paraformaldehyde to fix the cells does reduce the quality of preservation of internal cell structures, and hence is not suitable in all situations.

Figure 2. Visualization of the lysosomal compartment in bloodstream form *T. brucei*. The lysosome in trypanosomatids tends to be found as a single large structure or vacuole. This is clearly seen in the majority of the cells in this figure, where a single spot of fluorescence corresponding to the lysosome is detected between the nucleus and kinetoplast. Note the position of this structure is similar to that obtained with Concanavalin A at 37°C. **A:** Fluorescence channels of cells stained with lysotracker as described in the text. Red: lysotracker; blue: DAPI. **B:** Corresponding phase contrast image. Scale bar = 1.5 μm.

Figure 3. FM4-64 may be used to monitor both endocytosis and membrane recycling in *T. brucei*. Cells fed FM 4-64 were fixed at various times and prepared for immunofluorescence. **A:** Time course for FM 4-64 accumulation into the endosomal system. **B:** the recycling phase of the endosomal pathway. Cells preloaded with FM 4-64 are chased in medium in the absence of the stain. In both panels, the top row of images are fluorescence, FM 4-64 in red, DAPI in blue. Cells were treated for increasing times (left to right) as indicated at the bottom (in minutes 0, 0.5, 1.0, 2.0, 5.0, and 10). Scale bar = 2 μm.

Figure 4. Use of Concanavalin A to monitor endosomal compartments in bloodstream form *T. brucei*. A selection of images showing the differential staining that is achievable by incubation of trypanosomes with Concanavalin A at different temperatures. At 4°C, while the capping reaction is still possible, endocytosis is blocked, and hence the lectin accumulates within the flagellar pocket. This organelle is located close to the kinetoplast (small blue dot in the fluorescence images). Note the top cell in the 4°C specimen is in late mitosis, and both of the daughter flagellar pockets have been labeled with ConA. When incubated at 12°C, lectin is endocytosed, but retained within the early endosome (collecting tubules/TbRAB5A compartment). This structure is observed as a set of vesicles located between the flagellar pocket and the nucleus. Finally, at 37°C, ConA is able to gain access to the lysosome, most clearly observed in the lower cell in the 37°C panel, where the lectin is localized to a large nearly spherical structure. In each case, the phase image is at left, and the merge of the fluorescence signals obtained is at right (blue: DAPI, green: concanavalin A). The scale bar (bottom left) = 1.5 μm.

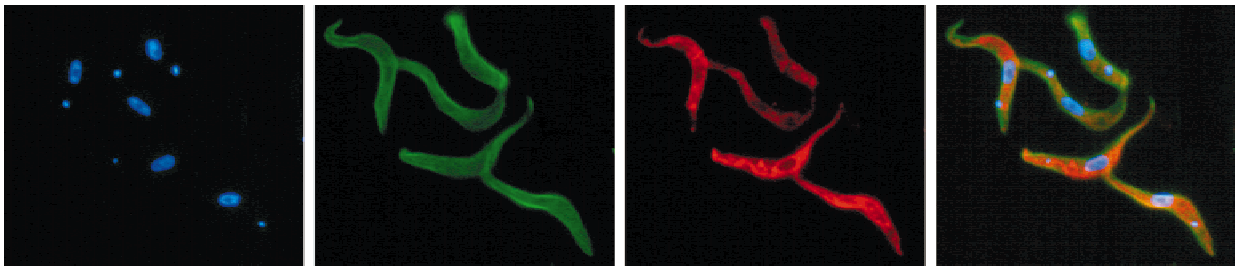

Figure 5. The endoplasmic reticulum in procyclic stage *T. brucei*. Transgenic procyclic form parasites, expressing an ectopic copy of TbRAB2, visualized by immunofluoresence. Green: tubulin; red: TbRAB2; blue: DAPI. Note that the endoplasmic reticulum extends throughout the cytoplasm as a network. The tubulin is mainly visualized as the subpellicular array surrounding the cell body. Note that despite the population of cells having been derived from a single cell, by limiting dilution, that expression of TbRAB2 is nonuniform, with some cells expressing substantially more of this antigen than others.

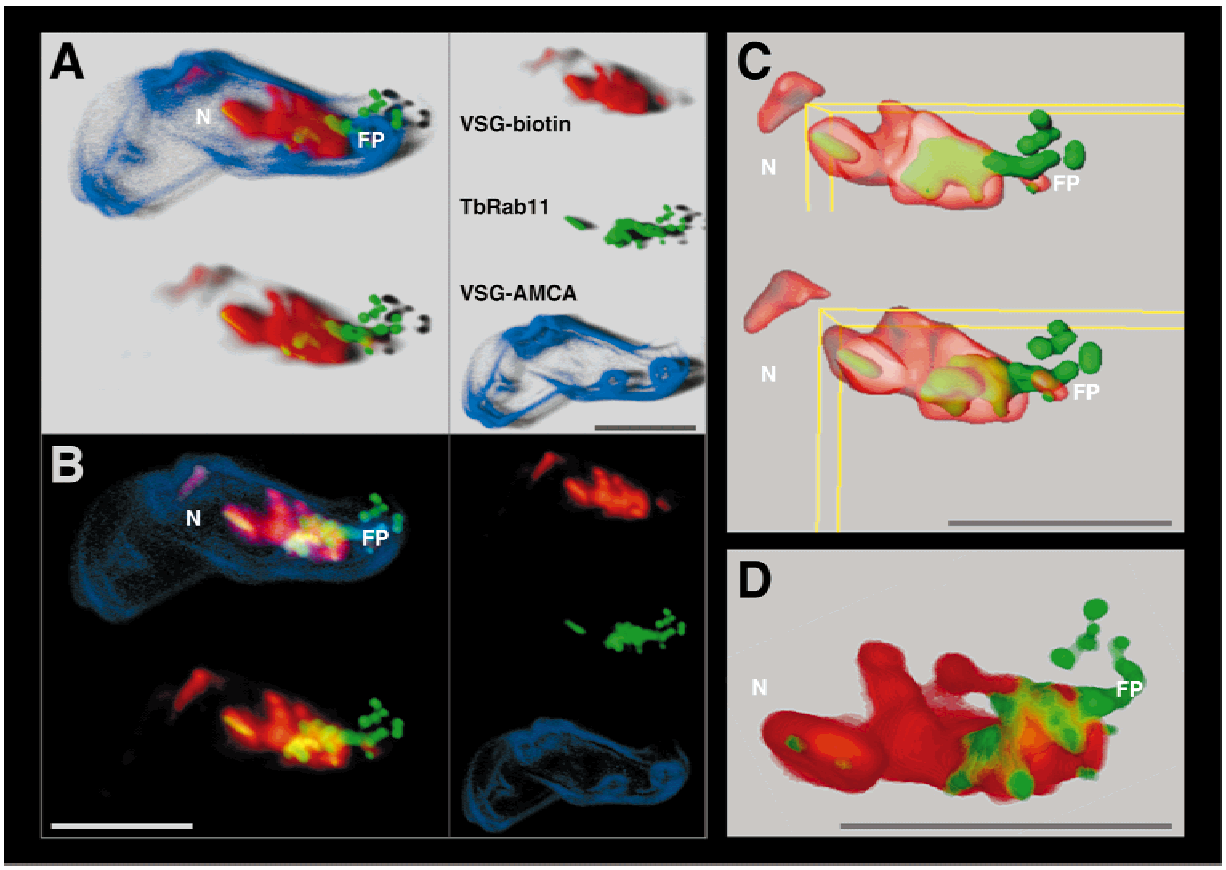

Figure 6. Distribution of endocytosed VSG and TbRab11 in bloodstream stage *T. brucei*. Live cells were surface labeled with Sulfo-NHS-SS-biotin and AMCA-Sulfo-NHS. Following endocytosis for 30 s at 37°C, cell surface bound biotin was removed by treatment with glutathione, and endocytosed VSG was detected in fixed and permeabilized cells by staining with Alexa Fluor™ 594 conjugated streptavidin (red). AMCA fluorescence (blue) was exclusively visible on the cell surface. TbRab11 was detected with a polyclonal rabbit antiserum, using Alexa Fluor™ 488 conjugated goat-anti-rabbit IgG as second antibody (green). Following digital deconvolution of multichannel 3D microscopic images with the Huygens software (SVI), visualization and analysis of the spatial fluorescence distribution and colocalization was done using the Imaris Surpass software (Bitplane). As the result of quantitative colocalization analysis, a single representative cell was chosen to illustrate the distribution of TbRab11 with respect to endocytosed VSG. The top right images in **A** and **B** represent the merged, summed 3D data. The bottom right images illustrate the colocalization of VSG-biotin (red) and TbRab11 (green). The different image channels are shown on the right (reduced to 66% size). The positions of the nucleus (N) and flagellar pocket (FP) are indicated. Scale bars = 3 μm. **A:** The shadow projection reveals the 3D spatial

Vital Stains for Intracellular Compartments

Lysotracker

Lysotracker dyes (Molecular Probes) are cell permeant acidotropic fluorphores that accumulate specifically in acidic organelles (Fig. 2). Lysotracker Red DND-99 is more useful than Lysotracker Green DND-26 because the latter tends to cause alkalinization of the lysosome and can only be used for very rapid labeling. By contrast, *T. brucei* can be incubated for several hours in the presence of Lysotracker Red, allowing a higher level of accumulation and giving a stronger signal than the green dye. Both dyes can be used to visualize lysosomes in live cells, but Lysotracker Red staining is more stable after fixation with paraformaldehyde (see Fig. 2). Lysotracker has been used to follow the disruption of the lysosome induced by TNF-α in *T. brucei* BSF (Magez et al., 1997).

Log phase BSF are harvested and resuspended at a concentration of 1×10^7/ml in complete HMI9 medium containing 50 nM Lysotracker Red DND-99. Cells are incubated with the dye for 30 min–1 h at 37°C. Labeling is stopped by the addition of paraformaldehyde to a final concentration of 4%. The cells are fixed for 1 h at 4°C as for regular IFA, washed in PBS, and adhered to Poly-L-Lysine slides for 30 min.

MitoTracker

MitoTracker was first applied to trypanosome studies by Vassella et al. (1997). Specific stains for the mitochondrion rely on the ΔpH gradient for targeting, but once fixed, this gradient will normally collapse, leading to diffusion of the stain. MitoTracker probes (Molecular Probes) are, however, retained by the mitochondrion following both fixation and permeabilization. MitoTracker probes are cell-permeant mitochondrion-selective dyes and contain a thiol-reactive chloromethyl moiety, which appears to be responsible for maintaining association with the mitochondria after fixation. There are several MitoTracker variants available, but the one best characterized is MitoTracker Red CMXROS (cat no. M-7512). This product is conveniently stored at 1 mM in DMSO, dessicated at −20°C and protected from sunlight. It is important to avoid repeat freeze thawing.

Cells are stained as follows. Harvest 10^6 mid log phase cells in a bench top centrifuge at $800 \times g$ for 10 min at 20°C in a 15-ml falcon tube. Add 1 μl of the 1 mM MitoTracker stock to 1 ml of serum-free HMI-9 prewarmed to 37°C (to a final concentration of 1 μM). Then, resuspend cells in 100 μl of the MitoTracker-containing media and incubate for 30 min in normal growth conditions (37°C, 5% CO_2 for bloodstream forms, 27°C for procyclics). In the case of bloodstream forms the lid of the falcon tube must be removed to allow CO_2 exchange. It is important that this step is adhered to as the accumulation of MitoTracker is reliant on the cells being fully energized. Add 1 ml of ice-cold 0.1% glucose in PBS to the falcon tube and transfer to a 1.5-ml microfuge eppendorf, and pellet the cells at 14,000 rpm for 20 s in a microfuge at 4°C (in a cold room). Aspirate and resuspend the cell pellet in 200 μl of PBS/0.1% glucose. Adhere cells to poly-L-lysine slides for 10 min in the dark at 4°C, using a PAP pen if required, and fix in 200 μl 4% paraformaldehyde/vPBS for 10 min at room temperature. Finally, wash in PBS for 2 min at 50 rpm using a Coplin jar on a rotator, and mount as for IFA. It is important to view the slide immediately as the stain is not well retained for extended periods after fixation.

Specific Endocytosis Stains

Specific staining of endocytic compartments and measurement of this process frequently requires a temperature blockade. Capping and endocytosis are extremely rapid in the BSF, with the result that both of these processes are difficult to fully inhibit by low temperature. A major pitfall of the methods below is inattention to the temperature parameter, and we therefore recommend that this is strictly adhered to, including chilling of all plasticware (including pipette tips), and working in a cold room.

FM4-64

FM4-64 is one of a family of styryl lipophilic dyes produced by Molecular Probes. The longwave red fluorescence of the

distribution of TbRab11 and endocytosed VSG. Shadow projection is a ray-tracing technique that uses artificial lights to illuminate structures. A viewing ray is sent through the volume image and evaluates which voxel can be seen to which degree using the principle of the simulated fluorescence process (SFP). Light directions and point of view can be altered to allow visualization of cells from different sides. **B:** Maximum Intensity Projection (MIP) is a volume-rendering technique that is commonly used for the two-dimensional presentation of 3D data sets. At each pixel the highest data value encountered along the corresponding viewing ray is determined. **C:** Surface rendering results in a transparent view of the areas occupied by VSG and Rab11. This technique is particularly useful for the analysis of structures that, in part, overlap. The viewing angle and magnification can be arbitrarily chosen. **D:** Transparency blending is a volume-rendering technique that applies the transparency information of the 3D data set to blend all values along the viewing direction. Volume rendering does not use intermediate geometrical representations, in contrast to surface-rendering techniques. It offers the possibility for displaying weak or fuzzy structures.

dye is markedly enhanced through membrane association. Low background levels minimize the need for washing and allow live cell imaging. Binding to membranes is rapid and reversible, so that the dye can be used as a marker for both endocytosis and membrane recycling (Fig. 3). FM4-64 has proved a useful tool in the study of the endocytic pathway in yeast and mammalian cells. In BSF, FM4-64 is primarily visible in the flagellar pocket at 4°C (see Fig. 3). Internalized material can be seen within 30 s. Intracellular staining increases with time, reaching a maximum at about 5 min. FM4-64 is nontoxic and cells can be incubated for several hours in the presence of the dye, leading to a generalized labeling of intracellular compartments. FM4-64 can also be used to follow recycling in *T. brucei*. After brief labeling of cells followed by reincubation in dye-free medium, FM4-64 staining is lost as the dye is recycled out of the cell (Fig. 3). Other lipophilic dyes may be also be useful in *T. brucei*: A related dye, FM2-10, is also an effective marker for endocytosis in BSF. As well as being a good general marker for endocytic compartments in BSF, FM4-64 is also useful for detecting uptake in the much less endocytically active procyclic cells. The kinetics of labeling are much slower than for BSF and there is a higher background level of plasma membrane staining in these cells. However, the intensity of the signal is stronger than for any other available markers tested. A very good alternative is FM2-10, which is used in the same manner as FM4-64, and in some hands can provide superior images.

Log phase BSF are harvested and washed twice at room temperature in TES buffer (120 mM NaCl, 5 mM KCl, 3 mM $MgSO_4$, 16 mM Na_2HPO_4, 5 mM KH_2PO_4, 30 mM TES, 10 mM glucose, 0.1 mM adenosine). Cells are resuspended to a concentration of about 1×10^7 cells/ml and preincubated for 10 min at 4°C or 37°C. FM4-64 is stored in a 16-mM stock solution in DMSO. The stock solution is diluted to 400 μM in TES, then added to the cells at a final concentration of 40 μM. Uptake is stopped by placing the cells on ice and the cells are fixed in 4% paraformaldehyde for 1 h. The fixed cells are washed three times in PBS then adhered to poly-L-lysine-coated slides for 30 min. Slides are mounted with Vectastain containing DAPI (Vector Laboratories). For recycling assays, cells are labeled for 5 min as described, washed once in ice cold TES at 4°C and resuspended in fresh TES. After reincubation at 37°C, cells are fixed and prepared for microscopy as above. PCF labeling with FM4-64 is similar, but lower concentrations of dye (10–20 μM) may be used to reduce background levels. Cells are incubated at 27°C for 15–20 min to achieve significant uptake.

FITC-Concanavalin A

The lectin Concanavalin A (ConA) binds to exposed oligosaccharides in the flagellar pocket of *T. brucei* BSFs (Balber & Frommel, 1988; Brickman & Balber, 1990). Transport of membrane-bound ConA can be blocked at various endosomal compartments by incubation of these cells at the following temperatures: At 4°C ConA remains localized in the FP and does not enter the cell, at 12°C ConA is transported to the TbRAB5A early endosome (collecting tubules) and at 37°C, transport of ConA continues to the lysosome (Brickman et al., 1995). The method for monitoring ConA uptake by *T. brucei* BSFs described here is based on experiments performed by Brickman et al. (1995; Fig. 4).

Midlog phase cells are harvested by centrifugation at $800 \times g$, ambient temperature, 10 min. The cell pellet is resuspended at 1×10^7/ml in serum-free HMI9 supplemented with 1% bovine serum albumin (BSA), prewarmed to 37°C. The cells are preincubated for 30 min at the required temperature for the uptake assay; 4°C, 12°C, or 37°C. FITC-ConA (Vector Laboratories) is then added to the parasites at a final concentration of 5 μg/ml and the cells incubated for a further 30 min at the appropriate temperature. After incubation the cells are transferred to ice and all subsequent manipulations performed using prechilled buffers, on ice, in the cold room to prevent any increase in temperature resulting in continued intracellular transport. The parasites are pelleted by centrifugation at top speed in a microcentrifuge for 20 s at 4°C and then resuspended in 1 ml vBPS to remove excess unbound ConA. Following recentrifugation for 20 s in the microcentrifuge as before, the final cell pellet is fixed in 3% PFA/vPBS at 4°C for 1 h. Excess PFA is washed off in vPBS and the cells finally resuspended in vPBS and adhered to poly-L-lysine-coated slides (Sigma) at room temperature for 20 min. Unbound cells are washed off in PBS before mounting the slides as described for IFA above.

FITC Transferrin Uptake

Harvest midlog phase BSF cells and wash twice at room temperature in TES-1% BSA. For continuous uptake, resuspend in prewarmed TES-BSA at a concentration of 1×10^7/ml and incubate at 37°C for 20 min. Add 50 μg/ml FITC-Tf (Sigma). Incubate for various times (1–30 min) at 37°C. For pulse-chase, resupend cells in ice cold TES-BSA and add 50 μg/ml FITC transferrin. Incubate for 30 min at 4°C to occupy surface receptors, then spin down and wash twice in TES-BSA. Resupend in TES-BSA and incubate at 37°C. In both cases, stop by the addition of 10 volumes ice cold vPBS. Spin down parasites at 4°C, resuspend in vPBS, and add paraformaldehyde to a final concentration of 4%. Incubate 1 h on ice, wash twice in PBS, and adhere to slides for 30 min at room temperature. After aspiration, slides may be mounted immediately or further processed for IFA.

FITC Tomato Lectin

Recently the polylactosamine-specific lectin from tomato (*Lycopersicum* spp.) was demonstrated to recognize specific glycan structures associated with the endocyctic system,

presumably components of resident endosomal glycoproteins (Nolan et al., 1999). Despite the fact that the precise determinants that the lectin recognizes have not been determined, the lectin is an excellent tool for visualizing the early endosomes (Nolan et al., 1999; Pal et al., 2002). The protocol below is designed to label primarily early endosomes, using a temperature block. This procedure results in superior image quality over direct staining of fixed cells.

Midlog phase trypanosomes ($\sim 10^6$ cells) are harvested by a bench top centrifuge at 800 $\times$ *g* for 10 min at 20°C. Cells are then washed with serum-free HMI-9 medium and resuspended in 100 μl of prewarmed serum-free HMI-9 containing 1 μl of FITC-tomato lectin (Sigma L-0401, stock solution at 1.4 mg/ml in 10 mM HEPES, 0.15 M NaCl, pH 7.5, containing 0.1 mM Ca^{2+} and 0.08% sodium azide). Uptake of the lectin is achieved by incubation of cells in the dark at 4°C for 10 min, followed by washing in vPBS. Cells are then incubated for a further 30-min period at 4°C and then pelleted by a spin at 14,000 rpm for 20 s. This final pellet is then resuspended in PBS, adhered to poly-lysine slides, and fixed and mounted as for IFA.

Other Compartments

Acidocalcisomes

This procedure is described by Docampo et al. (1995) and is adapted from a procedure for *Trypanosoma cruzi*. Log-phase parasites are washed three times by centrifugation at 800 $\times$ *g*, ambient temperature, 10 min, and the parasites resuspended in complete growth media (HMI-9 or SDM-79) containing 3 μM acridine orange (Sigma). The cells are then incubated for 10 min at the appropriate temperature (27°C or 37°C) with occasional gentle agitation. Excess acridine orange is removed by washing the parasites three times with PBS prior to fixation. This staining procedure provides a rather weak signal, and it is recommended that a high sensitivity camera be used, in addition to immediate viewing of the sample.

The Golgi Complex

The Golgi apparatus of *T. brucei* can be visualized using Bodipy-Texas Red ceramide (Molecular Probes; Field et al., 2000). A fluorescent ceramide:BSA conjugate is first prepared by dissolving the lipid in ethanol at 500 μM, followed by further dilution to 5 μM in a 1.8% solution (v/v) of defatted BSA (Sigma) in serum-free medium and incubation for 1 h at 4°C. Trypanosomes are incubated at 4°C for 1 h with the conjugated probe, washed, and incubated for 30 min at the growth temperature. This step serves to allow the cell to accumulate the probe in the Golgi complex, and if omitted, results in cells with extensively labeled internal membranes. The cells are then back-extracted twice with serum-free medium supplemented with 1.8% defatted BSA prior to fixation.

The Cytoskeleton

The trypanosome is a highly polarized cell, the structure of which is defined by a complex subpellicular array of highly cross-linked microtubules and provides an amenable system to investigate membrane/cytoskeletal interactions. The stability of the subpellicular array enables the trypanosomal microtubule cytoskeleton to be isolated intact using simple nonionic detergent extraction procedures (Robinson & Gull, 1991). This procedure effectively removes cytosolic and membrane-associated material leaving a microtubule cytoskeleton or "ghost" preparation that retains the shape and form of intact trypanosomes and can be readily visualized using light or electron microscopy (Robinson & Gull, 1991). Methods for the preparation of trypanosomal cytoskeletons have been extensively detailed; here a method exploiting Nonidet P-40 extraction is described (Robinson & Gull, 1991).

Trypanosomes are harvested at 1,000 $\times$ *g* at 4°C for 10 min, washed in vPBS, and repelleted. Cell pellets are gently resuspended in PEME buffer (0.1 M PIPES, pH 6.9, 2 mM EGTA, 1 mM $MgSO_4$, 0.1 mM EDTA) containing 1% (v/v) Nonidet P-40. The cells are then incubated on ice for 5 min. The ghost preparations are then extensively washed, first in PEME/Nonident P-40 and then PBS to remove cytoplasmic contaminants prior to processing for light or electron microscopy as detailed elsewhere in this article. The resultant specimen retains overall cell shape, but is devoid of most membrane markers (Fig. 6).

Quantitative Fluorescence Microscopy; Not Only Nice Pictures but Neat Numbers

Any 3D image, if acquired correctly, represents a set of valid data and not just a picture. What questions in trypanosome cell biology can be addressed using 3D deconvolution microscopy? Recently, the steady-state distribution of VSG in BSF trypanosomes has been analyzed by segmentation techniques to measure areas and volumes of the cell surface and intracellular structures (Grünfelder et al., 2002). The image was segmented using the edge criterion, based on the intensity properties of the structure, resulting in a masked image with four to seven separate objects. The largest object was verified as the cell surface. The summed fluorescence intensity in all voxels (3D pixels) of the cell surface object was calculated and compared to the summed voxel intensities of the other extracted objects. In this way the fluorescence distribution between cell surface and the intracellular compartments was determined. As a second criterion texture segmentation was used. This operation is based on the textural properties of fluorescent structures. For each of the voxels the variance of the analyzed neighborhood is computed, plus the square root of the variance (standard deviation) is calculated, resulting in a fine resolution of low intensity objects (due to the nonlinearity of the operation). This segmentation technique was used to separate the endo-

cytic compartments from the ER and Golgi. Finally, the summed fluorescence intensities of the three extracted objects (cell surface, endocytic compartment, and ER and Golgi) were compared. By extracting subregions of the perinuclear endoplasmic reticulum and the plasma membrane the VSG density gradient between these compartments was determined. As a proof of principle, the data obtained by digital segmentation analysis were challenged by two other methods (immunoelectron microscopy and differential biotinylation). All three methods yielded essentially the same results (Grünfelder et al., 2002). The application of quantitative fluorescence microscopy is not limited to highly abundant proteins as VSG. The described techniques have been successfully applied to studies on the cellular distribution of the *T. brucei* transferrin receptor (Mußmann et al., 2003) and a membrane-bound acidic phosphatase (F. Weise, M. Engstler, C.G. Grünfelder, & P. Overath, submitted) or for the quantification of sugars on the cell surface of insect stage trypanosomes (Vassella et al., 2003).

Besides measurement of protein abundance and concentration, it is most desirable to compare the localization of two or more proteins within a single cell. Colocalization analysis is frequently conducted by simply overlaying consecutively acquired images. This, however, only gives a crude estimate of the degree of colocalization and does not account for potential artefacts, resulting from, for example, pixel shifts. A valid quantification of multichannel colocalization signals can be digitally achieved using algorithms derived from flow cytometry software. Following color channel definition, a 3D histogram of the image is calculated and a polygonal region is selected. This region is chosen after creating a selection proposal from a restored data set with known colocalization. Threshold values and histogram regions are stored and applied for all images. After calculating the colocalization map, the colocalization voxels are extracted and statistically evaluated. This procedure has been successfully applied for the time-resolved analysis of VSG flow through distinct endosomal subcompartments of *T. brucei* (Grünfelder et al., 2003; Engstler et al., 2004), and the trafficking of EP procyclin during developmental transformation (Engstler & Boshart, 2004). Some specific examples of the methodology are described below.

Measurement of Recycling by Noninvasive, Chemical Tagging of the VSG Coat

The variant surface glycoprotein coat of *T. brucei* consists of 5×10^6 VSG dimers and only to about 5% of invariant proteins. Thus, *in vivo* labeling with sulfo-NHS-coupled reporter compounds can be regarded as a relatively VSG-specific stain. Small compounds such as biotin have the intrinsic advantage that they do not affect the properties of the tagged protein. An optimized protocol for biotinylation of bloodstream stage trypanosomes has recently been published (Grünfelder et al., 2002). The goal of the study was to measure the steady-state distribution of VSG and the protein density gradient between cell surface and intracellular compartments. For that purpose, a cleavable, membrane-impermeable derivative, sulfo-NHS-SS-biotin, was used. Cells were incubated on ice in a protein-free buffer with 1 mM biotinylation reagent (EZ-Link, Pierce), a concentration that assures that statistically all VSG molecules were biotinylated. Following endocytosis at 37°C, the surface biotin was cleaved off by addition of 50 mM glutathione and the cells were permeabilized. The internalized VSG was detected with streptavidin conjugates and located to the endosomal compartment. The quantitative analysis of VSG endocytosis by flow cytometry and quantitative electron and fluorescence microscopy gave essentially identical results (Grünfelder et al., 2002).

VSG Trafficking Close to the Flagellar Pocket

The high abundance of VSG greatly facilitates the analysis of protein trafficking from the place of biosynthesis, the perinuclear ER, to the cell surface. Probably one of the most interesting regions of the trypanosomal cell, the flagellar pocket is difficult to access by antibodies due to the carbohydrate-rich, gel-like matrix that fills the pocket lumen. To distinguish the flagellar pocket membrane from proximal VSG-containing endosomes is most important for the description of early and late events during VSG recycling. Dual staining of live cells with cleavable sulfo-NHS-SS-biotin and noncleavable sulfo-succinimidyl-7-amino-4-methylcoumarin-3-acetic acid (sulfo-NHS-AMCA) allows separation of surface-bound VSG from recycling VSG (Grünfelder et al., 2003; Engstler et al., 2004). Interestingly, the blue fluorescence of the methylcoumarin derivative is quantitatively quenched when VSG molecules are incorporated into endosomes. Thus, the cells reveal blue AMCA fluorescence at the cell surface, including the flagellar pocket membrane, and allow specific detection of recycling VSG with fluorophore-conjugated streptavidin after cleavage of surface biotin. An example of this type of staining is shown in Figure 6.

VSG Exocytosis

Compared to the analysis of VSG endocytosis, the measurement of VSG exocytosis has proven to be more difficult. The problem is distinguishing between surface VSG and protein that has reentered the cell surface after exocytosis. This can be overcome by generating a transgenic cell line expressing an epitope-tagged VSG. The TY1-tag is ideal as it is exposed at the N terminus of VSG221 and is accessible to an antipeptide antibody. Following endocytosis at 37°C, cells are acetylated on ice using sulfo-NHS-acetate as a substrate, a procedure that quantitatively blocks the binding of the anti-N-terminus antibody to the cell surface. Thus, upon exocytosis nonacetylated VSG is recycled from endosomes to the cell surface, where it is readily and specifically detect-

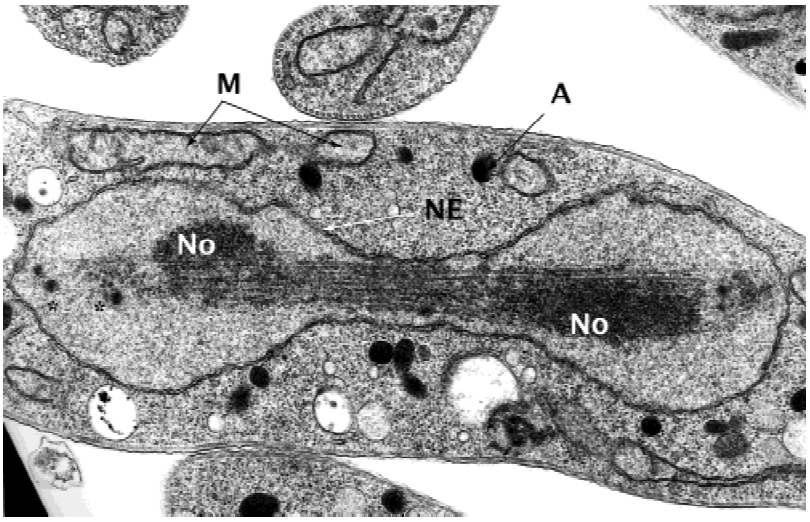

Figure 7. Ultrastructural image of the nuclear region of procyclic *T. brucei* undergoing mitosis. In this image the internal nuclear spindle is clearly visible passing through the central constriction between the two separating nuclei, as is the electron-dense nucleolus associated with the spindle (No). At the distal areas of the nucleus the kinetochores are also visible as dense structures (*), but the chromosomes themselves are not visualized. Note the double membrane of the nuclear envelope (NE). A portion of the mitochondrion is also visible (M) as are a number of highly electron-dense granules, most likely acidocalcisomes (A). Note the subpellicular array of microtubules that are visible in the cell at the top of the image as a regular pattern of small oval figures just below the plasma membrane. Magnification 50,000×.

able with the antipeptide antibody by flow cytometry and immunofluorescence microscopy.

Electron Microscopy

Despite the major advances in resolution that have been obtained recently at the light level, in the small trypanosome cell, where the majority of organelles are clustered within a portion of the cytoplasm that corresponds to ~30% of the total volume, definitive localization frequently requires ultrastructural detail (Fig. 7). Methods for regular transmission and immunoEM of cryo-frozen sections are described. A recent technique, involving high pressure rapid freezing of specimens, has been described for trypanosomatids, and which provides superb preservation of membrane structures (Grünfelder et al., 2002). This is a somewhat specialist application, but the interested reader is refered to the original article for technical details.

Transmission EM

Trypanosomes are fixed in suspension directly from the growth media by adding chilled 5% glutaraldehyde (TAAB, UK) and 8% paraformaldehyde (Sigma) in PBS (Sigma; tablet form) in a 1:1 ratio to the medium. The final composition of the fixative is therefore 2.5% glutaraldehyde/4% paraformaldehyde. Cultures are best analyzed when in mid-log phase, but this is not always possible; most important is that the fixation is achieved rapidly. Cells are fixed on ice for 10 min, centrifuged at 10,000 rpm for 5 min in 2-ml eppendorfs, and the supernatant carefully replaced with fresh fixative for a further 50 min without disturbing the pellet. This final pellet is then rinsed in 0.1 M sodium cacodylate and postfixed in 1% osmium tetroxide (TAAB, UK) in the same buffer at room temperature for 1 h. After rinsing in buffer, cells are then dehydrated in an ethanol series (20%, 30%, 50%, 70%, 90%, 95%, 100%, 100%, 100% ethanol each for 20 min), adding 1% uranyl acetate at the 30% stage, followed by propylene oxide, and then embedded in Epon/Araldite 502 (TAAB, UK) and finally polymerized at 60°C for 48 h.

Processing for Cryosections

Cells are fixed in suspension by adding chilled 0.4% glutaraldehyde and 8% paraformaldehyde in PBS in a 1:1 ratio to the growth medium containing trypanosomes to give final dilutions of 0.2% glutaraldehyde and 4% paraformaldehyde. Again the cells are fixed for 10 min on ice, then centrifuged and the supernatant replaced with fresh fixative for a further 50 min on ice to fully fix the pellet. The cells are then rinsed gently three times in ice-cold PBS over 15 min, then infused with cold freshly prepared 2.3 M sucrose in PBS in a 4°C refrigerator for between 8 h to overnight. Pieces of the pellet are then mounted in fresh sucrose solution on aluminum pins (Leica), plunge frozen into liquid nitrogen and stored. Eighty-nanometer cryosections can be cut from these pellets on a Leica FCS Ultracut T using a dry diamond knife, collected onto plastic loops containing 2.3 M sucrose in PBS, and transferred to form var-coated glow-discharged 200 hexagonal mesh copper/palladium grids (Agar Scientific) for immunogold labeling (see below).

Immunogold Labeling

On a strip of Parafilm placed along the laboratory bench, the grids from the procedure above are transferred section-side down onto drops of 0.05 M glycine for 5 min to block free aldehyde groups within the fixed cells and then into 5% or 10% fetal calf serum in PBS (in which blocking medium all subsequent reagents were diluted) for 20 min. The grids are then moved along from drop to drop in rabbit primary antibody 0.5–500 μg/ml for 1 h, rinsed 3 times for 5 min

each in PBS, incubated in protein-A gold (Department of Cell Biology, University Medical Center, Utrecht, Netherlands) for 45 min, rinsed 5 times in PBS for 5 min each, fixed in 2.5% glutaraldehyde in PBS for 10 min, rinsed 10 times in freshly distilled water over 10 min to remove phosphate, contrasted on drops of 2% methyl cellulose and 0.3% uranyl acetate on an ice-chilled metal block in the dark for 10 min, picked up on wire loops, and blotted dry. The above technique for preparing cryosections and for immunogold labeling is described in detail in Slot et al. (1991).

Acknowledgments

The Imperial College laboratory is supported by the Wellcome Trust. We are grateful to our collaborators for the provision of a number of original protocols described here. M.E. acknowledges Michael Boshart for the continuous support in his laboratory and Peter Overath for most influential discussion. M.E. is supported by the DFG (grant EN305/2).

References

Agabian, N. (1990). *Trans*-splicing of nuclear pre-mRNAs. *Cell* **61**, 1157–1160.

Ali, B.R., Pal, A., Croft, S.L., Taylor, R.J. & Field, M.C. (1999). The farnesyltransferase inhibitor manumycin A is a novel trypanocide with a complex mode of action including major effects on mitochondria. *Mol Biochem Parasitol* **104**, 67–80.

Allen, C.L., Goulding, D. & Field, M.C. (2003). Clathrin-mediated endocytosis is essential in *Trypanosoma brucei*. *EMBO J* **22**, 4991–5002.

Armstrong, J.A., Brown, K.N. & Valentine, R.C. (1964). The ingestion of protein molecules by blood forms of *Trypanosoma* rhodesiense. *Trans Roy Soc Trop Med Hyg* **58**, 291.

Balber, A.E. & Frommel, T.O. (1988). *Trypanosoma brucei gambiense* and *T. b. rhodesiense*: Concanavalin A binding to the membrane and flagellar pocket of bloodstream and procyclic forms. *J Protozool* **35**, 214–219.

Bangs, J.D. (1998). Surface coats and secretory trafficking in African trypanosomes. *Curr Opin Microbiol* **1**, 448–454.

Bangs, J.D., Brouch, E.M., Ransom, D.M. & Roggy, J.L. (1996). A soluble secretory reporter system in *Trypanosoma brucei*. Studies on endoplasmic reticulum targeting. *J Biol Chem* **271**, 18387–18393.

Beverley, S.M. (2003). Protozomics: Trypanosomatid parasite genetics comes of age. *Nat Rev Genet* **4**, 11–19.

Brickman, M.J. & Balber, A.E. (1990). *Trypanosoma brucei rhodesiense* bloodstream forms: Surface ricin-binding glycoproteins are localized exclusively in the flagellar pocket and the flagellar adhesion zone. *J Protozool* **37**, 219–224.

Brickman, M.J., Cook, J.M. & Balber, A.E. (1995). Low temperature reversibly inhibits transport from tubular endosomes to a perinuclear, acidic compartment in African trypanosomes. *J Cell Sci* **108**, 3611–3621.

Bruce, D. (1911). The morphology of *Trypanosoma evansi* (Steel). *Proc Roy Soc B* **84**, 181.

Bruce, D. (1915). The Croonian lectures on trypanosomes. *Lancet* June 26, 1323–1330.

Cross, G.A.M. (1996). Antigenic variation in trypanosomes: Secrets surface slowly. *Bioessays* **18**, 283–291.

Denny, P.W., Gokool, S., Russell, D.G., Field, M.C. & Smith, D.F. (2000). Acylation-dependent protein export in Leishmania. *J Biol Chem* **275**, 11017–11025.

Docampo, R. & Moreno, S.N. (1999). Acidocalcisome: A novel Ca^{2+} storage compartment in trypanosomatids and apicomplexan parasites. *Parasitol Today* **15**, 443–448.

Docampo, R., Scott, D.S., Vercesi, A.E. & Moreno, S.N.J. (1995). Intracellular Ca^{2+} storage in acidocalcisomes of *Trypanosoma cruzi*. *Biochem J* **310**, 1005–1012.

Engstler, M. & Boshart, M. (2004). *Genes & Development* (in press).

Engstler, M., Thilo, L., Weise, F., Grünfelder, C.G., Schwarz, H., Boshart, M. & Overath, P. (2004). Kinetics of endocytosis and recycling of the GPI-anchored variant surface glycoprotein in *Trypanosoma brucei*. *J Cell Sci* **117**, 1105–1115.

Engstler, M., Weise, F., Bopp, K., Gruenfelder, C.G. & Overath, P. (2004). *Molec Microbiol* (in press).

Ferguson, M.A.J. (1999). The structure, biosynthesis and functions of glycosylphosphatidylinositol anchors, and the contributions of trypanosome research. *J Cell Sci* **112**, 2799–2809.

Field, H., Ali, B.R., Sherwin, T., Gull, K., Croft, S.L. & Field, M.C. (1999). TbRab2p, a marker for the endoplasmic reticulum of *Trypanosoma brucei*, localises to the ERGIC in mammalian cells. *J Cell Sci* **112**, 147–156.

Field, H., Farjah, M., Pal, A., Gull, K. & Field, M.C. (1998). Complexity of trypanosomatid endocytosis pathways revealed by Rab4 and Rab5 isoforms in *Trypanosoma brucei*. *J Biol Chem* **273**, 32102–32110.

Field, H., Sherwin, T., Smith, A.C., Gull, K. & Field, M.C. (2000). Cell-cycle and developmental regulation of TbRAB31 localisation, a GTP-locked Rab protein from *Trypanosoma brucei*. *Mol Biochem Parasitol* **106**, 21–35.

Gull, K. (1999). The cytoskeleton of trypanosomatid parasites. *Annu Rev Microbiol* **53**, 629–655.

Grünfelder, C.G., Engstler, M., Weise, F., Schwarz, H., Stierhof, Y.D., Boshart, M. & Overath, P. (2002). Accumulation of a GPI-anchored protein at the cell surface requires sorting at multiple intracellular levels. *Traffic* **3**, 547–559.

Grünfelder, C.G., Engstler, M., Weise, F., Schwarz, H., Stierhof, Y.D., Morgan, G.W., Field, M.C. & Overath, P. (2003). Endocytosis of a GPI-anchored protein via clathrin-coated vesicles, sorting by default in endosomes and exocytosis via TbRAB11-positive carriers. *Mol Biol Cell* **14**, 2029–2040.

Hoare, C.E. (1972). *The trypanosomes of mammals; a zoological monograph*. Oxford: Blackwell Scientific Publications.

Jeffries, T.R., Morgan, G.W. & Field, M.C. (2001). A developmentally regulated rab11 homologue in *Trypanosoma brucei* is involved in recycling processes. *J Cell Sci* **114**, 2617–2626.

Jeffries, T.R., Morgan, G.W. & Field, M.C. (2002). TbRAB18, a developmentally regulated Golgi GTPase from *Trypanosoma brucei*. *Mol Biochem Parasitol* **121**, 63–74.

Kable, M., Heidmann, S. & Stuart, K. (1997). RNA editing: Getting the U into RNA. *Trends Biochem Sci* **22**, 162–166.

Kelley, R.J., Alexander, D.L., Cowan, C., Balber, A.E. & Bangs, J.D. (1999). Molecular cloning of p67, a lysosomal membrane glycoprotein from *Trypanosoma brucei*. *Mol Biochem Parasitol* **98**, 17–28.

Legros, D., Ollivier, G., Gastellu-Etchegorry, M., Paquet, C., Burri, C., Jannin, J. & Buscher, P. (2002). Treatment of human African trypanosomiasis—Present situation and needs for research and development. *Lancet Infect Dis* **2**, 437–440.

Lorenz, P., Maier, A.G., Baumgart, E., Erdmann, R. & Clayton, C. (1998). Elongation and clustering of glycosomes in *Trypanosoma brucei* overexpressing the glycosomal Pex11p. *EMBO J* **17**, 3542–3555.

Lukes, J., Guilbride, D.L., Votypka, J., Zikova, A., Benne, R. & Englund, P.T. (2002). Kinetoplast DNA network: Evolution of an improbable structure. *Eukaryot Cell* **1**, 495–502.

Magez, S., Geuskens, M., Beschin, A., del Favero, H., Verschueren, H., Lucas, R., Pays, E. & de Baetselier, P. (1997). Specific uptake of tumor necrosis factor-alpha is involved in growth control of *Trypanosoma brucei*. *J Cell Biol* **137**, 715–727.

Marchesini, N., Ruiz, F.A., Vieira, M. & Docampo, R. (2002). Acidocalcisomes are functionally linked to the contractile vacuole *of Dictyostelium discoideum*. *J Biol Chem***277**, 8146–8153.

McConville, M.J. & Ferguson, M.A. (1993). The structure, biosynthesis and function of glycosylated phosphatidylinositols in the parasitic protozoa and higher eukaryotes. *Biochem J* **294**, 305–324.

Minchin, E.A. (1909). The structure of *Trypanosoma lewisi* in relation to microscopical technique. *Q J Micr Sci* **53**, 755.

Morgan, G.W., Hall, B.S., Denny, P.W., Carrington, M. & Field, M.C. (2002*a*). The kinetoplastida endocytic apparatus. Part I: A dynamic system for nutrition and evasion of host defences. *Trends Parasitol* **18**, 491–496.

Morgan, G.W., Hall, B.S., Denny, P.W., Field, M.C. & Carrington, M. (2002*b*). The endocytic apparatus of the kinetoplastida. Part II: Machinery and components of the system. *Trends Parasitol* **18**, 540–546.

Mußmann, R., Jansen, H., Calafat, J., Engstler, M., Ansorge, I., Clayton, C. & Borst, P. (2003). The expression level determines the surface distribution of the transferrin receptor in *Trypanosoma brucei*. *Mol Microbiol* **47**, 1–23.

Nolan, D.P., Geuskens, M. & Pays, E. (1999). N-linked glycans containing linear poly-N-acetyllactosamine as sorting signals in endocytosis in *Trypanosoma brucei*. *Curr Biol* **9**, 1169–1172.

Nolan, D.P., Jackson, D.G., Biggs, M.J., Brabazon, E.D., Pays, A., Van Laethem, F., Paturiaux-Hanocq, F., Elliot, J.F., Voorheis, H.P. & Pays, E. (2000). Characterization of a novel alanine-rich protein located in surface microdomains in *Trypanosoma brucei*. *J Biol Chem* **275**, 4072–4080.

Ogbadoyi, E., Ersfeld, K., Robinson, D., Sherwin, T. & Gull, K. (2000). Architecture of the *Trypanosoma brucei* nucleus during interphase and mitosis. *Chromosoma* **108**, 501–513.

Opperdoes, F.R. & Michels, P.A.M. (1993). The glycosomes of the kinetoplastida. *Biochimie* **75**, 231–234.

Overath, P. & Engstler, M. (2004). Endocytosis, membrane recycling and sorting of GPI-anchored proteins: *Trypanosoma brucei* as a model system. *Mol Microbiol* **53**, 735–744.

Pal, A., Hall, B.S., Nesbeth, D.N., Field, H.I. & Field, M.C. (2002). Differential endocytic functions of *Trypanosoma brucei* Rab5 isoforms reveal a glycosylphosphatidylinositol-specific endosomal pathway. *J Biol Chem* **277**, 9529–9539.

Patnaik, P.K., Field, M.C., Menon, A.K., Cross, G.A., Yee, M.C. & Butikofer, P. (1993). Molecular species analysis of phospholipids from *Trypanosoma brucei* bloodstream and procyclic forms. *Mol Biochem Parasitol* **58**, 97–105.

Remme, J.H., Blas, E., Chitsulo, L., Desjeux, P.M., Engers, H.D., Kanyok, T.P., Kayondo, J.F., Kioy, D.W., Kumaraswami, V., Lazdins, J.K., Nunn, P.P., Oduola, A., Ridley, R.G., Toure, Y.T., Zicker, F. & Morel, C.M. (2002). Strategic emphases for tropical diseases research: A TDR perspective. *Trends Microbiol* **10**, 435–440.

Robinson, D.R. & Gull, K. (1991). Basal body movements as a mechanism for mitochondrial genome segregation in the trypanosome cell cycle. *Nature* **352**, 731–733.

Robinson, D.R., Sherwin, T., Ploubidou, A., Byard, E.H. & Gull, K. (1995). Microtubule polarity and dynamics in the control of organelle positioning, segregation, and cytokinesis in the trypanosome cell cycle. *J Cell Biol* **128**, 1163–1172.

Rout, M.P. & Field, M.C. (2001). Isolation and characterization of subnuclear compartments from *Trypanosoma brucei*. Identification of a major repetitive nuclear lamina component. *J Biol Chem* **276**, 38261–38271.

Slot, J.W., Geuze, H.J., Gigengack, S., Lienhard, G.E. & James, D.E. (1991). Immunolocalisation of the insulin regulatory glucose transporter in brown adipose tissue of the rat. *J Cell Biol* **113**, 123–135.

Tokuyasu, K.T. (1986). Application of cryoultramicrotomy to immunocytochemistry. *J Microsc* **143**, 139–149.

Tyler, K.M., Matthews, K.R. & Gull, K. (2001). Anisomorphic cell division by African trypanosomes. *Protist* **152**, 367–378.

Vassella, E., Bütikofer, P., Engstler, M., Jelk, J. & Roditi, I. (2003). Procyclin null mutants of *Trypanosoma brucei* express free GPIs on their cell surface. *Mol Biol Cell* **14**, 1308–1318.

Vassella, E., Straesser, K. & Boshart, M. (1997). A mitochondrion-specific dye for multicolour fluorescent imaging of *Trypanosoma brucei*. *Mol Biochem Parasitol* **90**, 381–385.

Vickerman, K. (1969*a*). On the surface coat and flagellar adhesion in trypanosomes. *J Cell Sci* **5**, 163–193.

Vickerman, K. (1969*b*). The fine structure of *Trypanosoma congolense* in its bloodstream phase. *J Protozool* **16**, 54–69.

Vickerman, K. (1970). Functional aspects of the cytology of trypanosomes. *Trans Roy Soc Trop Med Hyg* **64**, 180–181.

Wang, Z., Drew, M.E., Morris, J.C. & Englund, P.T. (2002). Asymmetrical division of the kinetoplast DNA network of the trypanosome. *EMBO J* **21**, 4998–5005.

Woodward, R., Carden, M.J. & Gull, K. (1995). Immunological characterization of cytoskeletal proteins associated with the basal body, axoneme and flagellum attachment zone of *Trypanosoma brucei*. *Parasitology* **111**, 77–85.